



## Single step synthesis of $\text{Li}_2\text{TiO}_3$ powder

Amit Sinha \*, S.R. Nair, P.K. Sinha

Energy Conversion Materials Section, Materials Group, Bhabha Atomic Research Centre, Vashi Complex, Navi Mumbai 400705, India

### ARTICLE INFO

#### Article history:

Received 5 October 2009

Accepted 15 January 2010

#### Keywords:

Synthesis

$\text{Li}_2\text{TiO}_3$

Ceramics

Sol–gel preparation

Sintering

Breeding materials

### ABSTRACT

A novel process method based on solid–liquid combustion synthesis has been developed to produce high purity monoclinic  $\text{Li}_2\text{TiO}_3$  directly after combustion. The process does not call for any additional heat treatment for phase formation. The lattice parameters of  $\text{Li}_2\text{TiO}_3$  were determined through Rietveld refinement of XRD pattern. Systematic studies were carried out to optimize the sintering temperature to obtain the desired microstructure and density in the sintered specimens. The morphology of  $\text{Li}_2\text{TiO}_3$  powder and microstructures of sintered specimens were studied by scanning electron microscopy. The powder produced through this route could be sintered to 90% of theoretical density at relatively low temperatures ( $<1150^\circ\text{C}$ ). The process developed in the present investigation is simple and convenient for mass production.

© 2010 Elsevier B.V. All rights reserved.

### 1. Introduction

In a fusion reactor, the breeder material plays an important role in producing tritium atoms by a lithium transmutation,  ${}^6\text{Li} + n \rightarrow {}^4\text{He} + \text{T}$ , where  $n$  is the neutron and  $\text{T}$  is the tritium. Hence, lithium based ceramics have been considered as candidate ceramic breeder materials for tritium breeding in both the helium cooled pebble-bed blanket for DEMO and the ITER breeding blanket due to their good thermal properties, especially high thermal conductivity, as well as satisfactory breeding characteristics [1,2]. Among these,  $\text{Li}_2\text{TiO}_3$  is considered as the leading candidate material because of its fairly good tritium release property at low temperatures between 200 and  $400^\circ\text{C}$  and its low activation characteristics [3–6].

There have been a number of reports in the literature on the preparation of  $\text{Li}_2\text{TiO}_3$  powder. Conventionally,  $\text{Li}_2\text{TiO}_3$  is produced by solid state reaction of a powder mixture of  $\text{Li}_2\text{CO}_3$  and  $\text{TiO}_2$  at  $750^\circ\text{C}$  for 10–20 h [4,7]. Deptula et al. [8] reported a sol–gel process for preparation of  $\text{Li}_2\text{TiO}_3$  starting from  $\text{LiOH}$  and commercially available  $\text{TiCl}_4$  as a source of lithium and titanium, respectively. However their process was cumbersome as they needed to dissolve  $\text{TiCl}_4$  in concentrated aqueous  $\text{HCl}$  followed by elimination of chloride ion by repeated distillation with nitric acid. Using citrate gel route, Alvani et al. [9] prepared  $\text{Li}_2\text{TiO}_3$  powder where the precursor powder yielded the phase after calcination at  $650^\circ\text{C}$ . A solution combustion synthesis of  $\text{Li}_2\text{TiO}_3$  starting with aqueous solutions of  $\text{LiNO}_3$  and  $\text{TiO}(\text{NO}_3)_2$  was described by Jung

et al. [10] However, the powder produced through this process could only be sintered to 80% T.D. at a temperature of  $1100^\circ\text{C}$  [10].

Solution combustion synthesis (SCS) is a noble powder preparation method for the preparation of high purity, sinter-active and nanocrystalline ceramic powders. In the SCS process, the precursor solution contains the oxidizers and the readily combustible fuel, which upon heating, after dehydration, the decomposition of nitrate takes place giving rise to evolution of oxides of nitrogen. The exothermic oxidation–reduction reaction of gas phases increases the temperature of the viscous mixture immediately adjoining the combustion zone. The reaction process proceeds rather rapidly and is sustained till the entire viscous mixture is consumed. The rapid rise in temperature during flame combustion, and the volume of gas generated during the combustion reaction depend on several factors such as type, composition and content of the fuel. It has been reported that a stoichiometric composition gives rise to higher temperatures and the evolution of more gases [11–14].

For synthesis of titanate based ceramics using SCS route, titanium ion is required to be in aqueous solution form. The various starting materials for titanium, which are commonly used in SCS, are  $\text{TiCl}_4$ ,  $\text{Ti}(\text{C}_6\text{H}_6\text{O}_7)_2$ ,  $\text{Ti}(\text{OC}_3\text{H}_7)_4$ ,  $\text{TiO}(\text{NO}_3)_2$ , etc. These compounds are either difficult to handle or too expensive, making the cost of production of the final product higher. In the present investigation,  $\text{Li}_2\text{TiO}_3$  powder was synthesized by a novel solid–liquid combustion synthesis (SLCS) using uncalcined hydrated titania powder and aqueous  $\text{LiNO}_3$  as the starting materials for titanium and lithium, respectively. Based on our literature survey, it is the first report on the synthesis of  $\text{Li}_2\text{TiO}_3$  powder directly after combustion reaction starting with  $\text{TiO}_2$  which calls for no further

\* Corresponding author. Tel.: +91 22 27887161; fax: +91 22 27840032.  
E-mail address: [amit97@yahoo.com](mailto:amit97@yahoo.com) (A. Sinha).

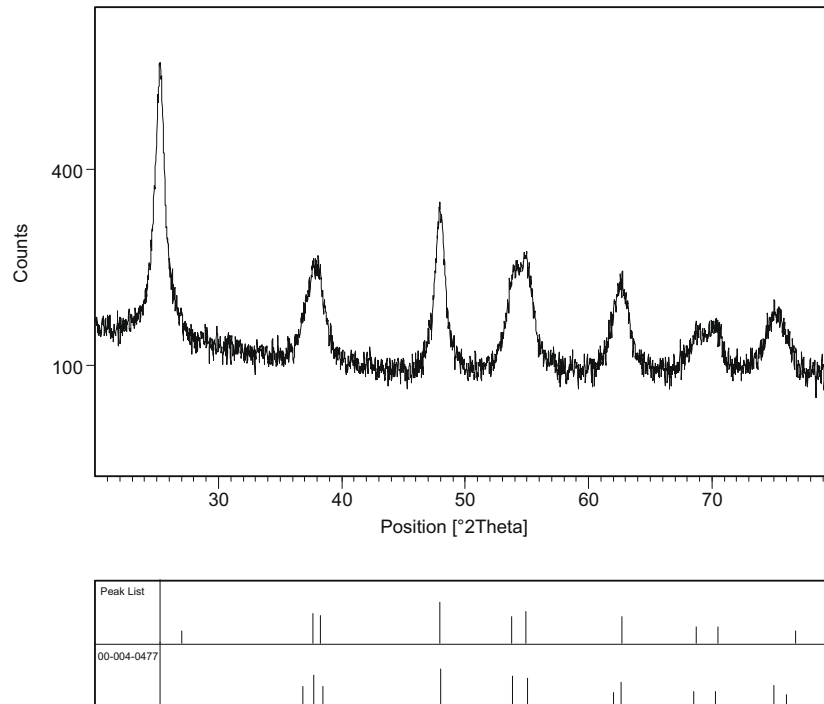


Fig. 1. XRD pattern of uncalcined hydrated titania powder.

calcination for phase formation. Systematic studies were carried out to optimize the sintering temperature to obtain the desired microstructure and density in the sintered specimens.

## 2. Experimental procedure

$\text{LiNO}_3$  (AR Grade, E-Merck, India), and uncalcined hydrated titania powder ( $\text{TiO}_2 \cdot x\text{H}_2\text{O}$  where  $x = 0.97$ ; M/s Travancore Titanium Products Ltd., India) were used as starting materials for the preparation of  $\text{Li}_2\text{TiO}_3$  powder. Equimolar amount of aqueous solution of  $\text{LiNO}_3$  was mixed with hydrated titania powder. In the solution ammonium nitrate was used in the form of an additional oxidizer. The metal ions were complexed by stoichiometric quantities of fuel (glycine) (AR Grade, E-merck, India). The mixed solution was slowly dehydrated under a hot plate to form a viscous, transparent gel wherein the titania powder was uniformly dispersed. With subsequent dehydration, a flame combustion reaction took place that yielded a white powder. The combustion reaction was completed in less than 10 s.

The powders obtained after combustion reaction were characterized by X-ray diffraction (Philips Analytical, Model PW1710) for phase analysis. A standard silicon sample supplied by the manufacturer was employed as internal standard for calibration. The XRD patterns were recorded at a scan rate of  $0.025^\circ/\text{s}$  using  $\text{Cu K}\alpha$  radiation. The lattice parameters of  $\text{Li}_2\text{TiO}_3$  were determined using Rietveld refinement on XRD data. Rietveld analysis was performed using Fullprof program incorporated in the WinPLOTR software package [15].

The as produced  $\text{Li}_2\text{TiO}_3$  powder after combustion synthesis was ground in a ball mill. The ground powder was compacted in a uniaxial hydraulic press at 150 MPa and subsequently sintered at  $1050\text{--}1200^\circ\text{C}$  for 90 min. The microstructural analysis of the sintered samples was carried out by scanning electron microscopy (SERON AIS2100). Cylindrical sintered specimens having diameter of 10 mm were used for measurement of density and open porosity using Archimedes water displacement technique.

## 3. Results and discussion

### 3.1. Synthesis of $\text{Li}_2\text{TiO}_3$ powder

Fig. 1 shows the XRD pattern of hydrated titania powder used for the preparation of lithium titanate in the present investigation. All the reflections of the pattern could be assigned to the anatase phase of  $\text{TiO}_2$  [ICDD PDF 004-0477]. From the X-ray line-broadening, the crystallite size of the powder was calculated. The calculated average crystallite size of the powder was 26.3 nm. The nano-crystallinity of starting powder is an important factor for obtaining the final phase after combustion synthesis.

The XRD pattern of the white powder produced after combustion starting with  $\text{LiNO}_3$  and hydrated titania is shown in Fig. 2. The reflections of the pattern correspond to monoclinic polymorph of  $\text{Li}_2\text{TiO}_3$  [ICDD PDF 033-0831].  $\text{Li}_2\text{TiO}_3$  exists in three polymorphic modifications, e.g.  $\alpha$ ,  $\beta$  and  $\gamma$  [16]. The low temperature  $\beta$ - $\text{Li}_2\text{TiO}_3$  phase is monoclinic, has a homogeneity range between 47 and 51 mol.%  $\text{TiO}_2$  [16] and crystallizes in the  $\text{Li}_2\text{SnO}_3$  type structure with the space group  $\text{C2/c}$  (no. 15) having a room temperature X-ray density of  $3.43\text{ g/cc}$  [17]. The high-temperature  $\gamma$ - $\text{Li}_2\text{TiO}_3$  phase is cubic and crystallizes in the NaCl type structure, which is having a broad homogeneity range between 43 and 64 mol.%  $\text{TiO}_2$  at these temperatures. The  $\beta$ - $\gamma$  transformation is reported to take place at a temperature greater than  $1150^\circ\text{C}$  [16,18,19]. The XRD results indicate that in the present investigation, the desired phase could be produced after combustion synthesis which calls for no further heat treatment for phase formation. Fig. 3 shows the SEM photomicrograph of as prepared  $\text{Li}_2\text{TiO}_3$  powder. It can be observed that the powder produced is coarse and is composed of hard-agglomerates. The sintering study of as produced powder at  $1200^\circ\text{C}$  for 90 min resulted in specimen with lower density (80% of the theoretical density). The lower sintered density of the product could be attributed to the presence of hard-agglomerates in the starting powder. In order to overcome the above problem, the as synthesized powder was wet-ball milled. Fig. 4 shows the SEM photomicrograph of the ground  $\text{Li}_2\text{TiO}_3$  powder. The average

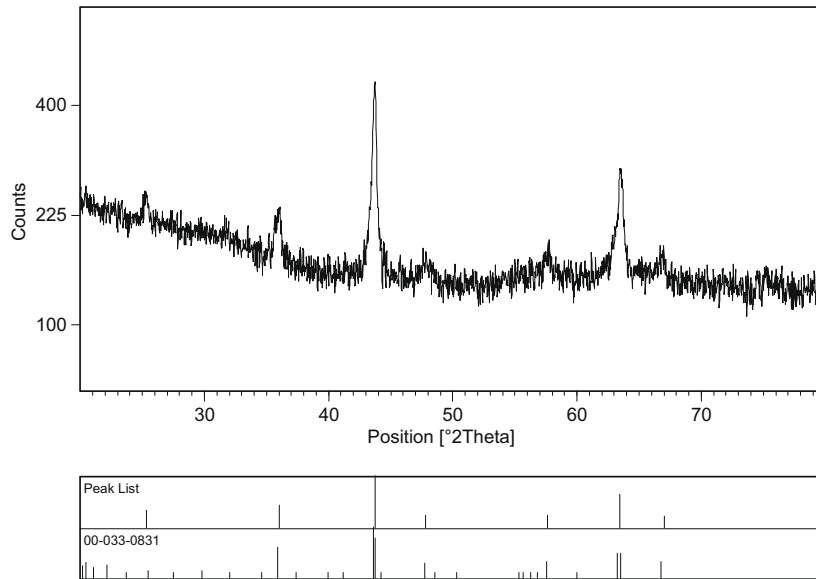


Fig. 2. XRD pattern of as synthesized  $\text{Li}_2\text{TiO}_3$  powder.

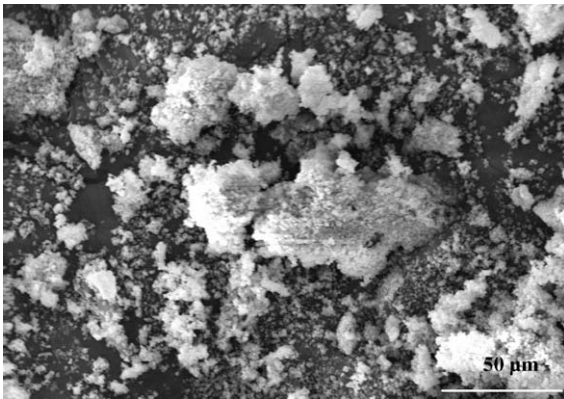


Fig. 3. SEM photomicrograph of as synthesized  $\text{Li}_2\text{TiO}_3$  powder.

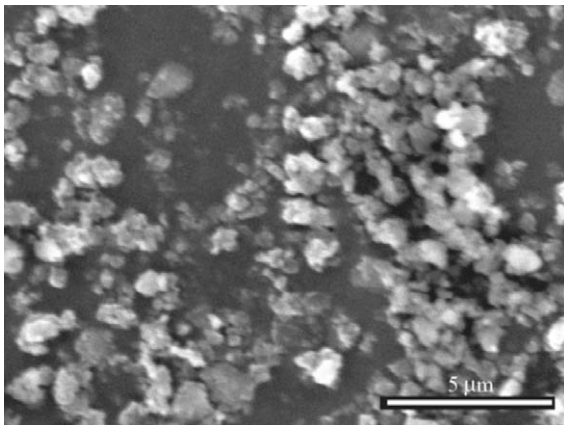


Fig. 4. SEM photomicrograph of  $\text{Li}_2\text{TiO}_3$  powder after ball milling.

powder particle size of the  $\text{Li}_2\text{TiO}_3$  powder after grinding was  $1\ \mu\text{m}$ .

### 3.2. Sintering behavior of $\text{Li}_2\text{TiO}_3$

The densification of  $\text{Li}_2\text{TiO}_3$  ceramic is difficult due to its fast grain growth behavior during sintering which results in several

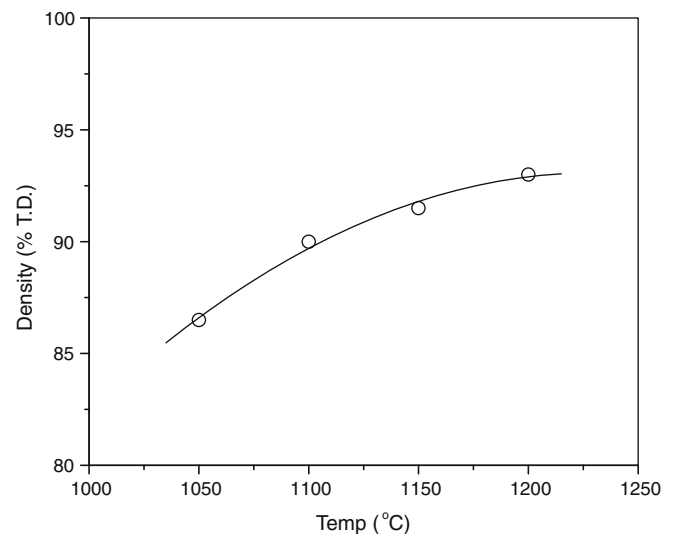
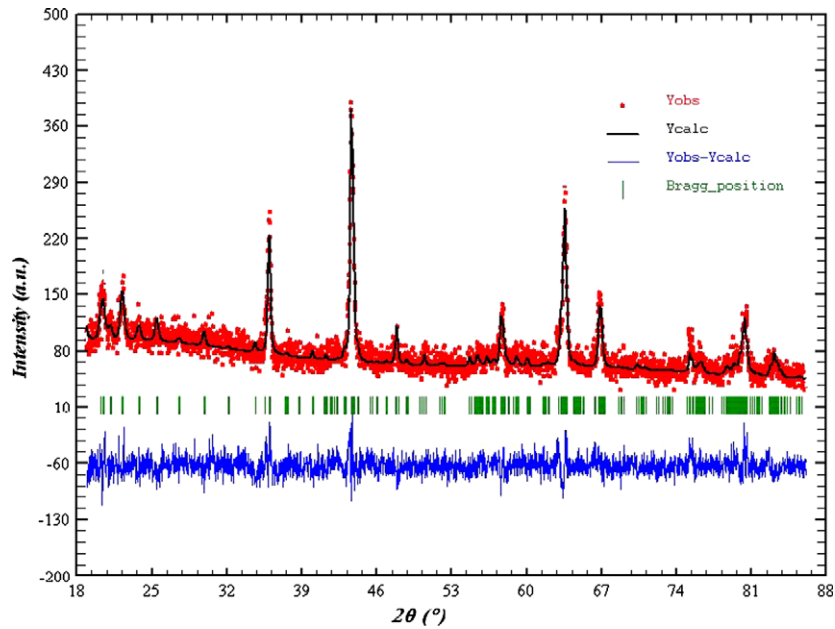
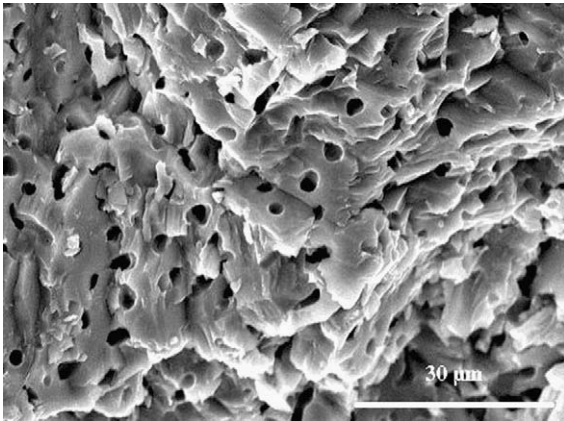


Fig. 5. Plot of sintered density of  $\text{Li}_2\text{TiO}_3$  as a function of sintering temperature.

large pore traps in over-sized grains or on grain boundaries. These entrapped pores do not get removed during any additional sintering process. So, densification should take place at a relatively low temperature before a rapid grain growth sets in [20]. Hence, in order to study the effect of sintering temperature on the densification behavior of milled  $\text{Li}_2\text{TiO}_3$  powder, the green compacts were sintered at temperatures varying from 1050 to 1200 °C, respectively. The relative densities of the sintered pellets are shown in Fig. 5. In general, the increase of sintering temperature increases the density of the compacts. It can be observed from Fig. 5 that the compacts could be sintered to 90% TD at 1100 °C which is comparable to the density obtained by rapid sintering [21]. At higher sintering temperature, the sintered density increased marginally. Sintering of  $\text{Li}_2\text{TiO}_3$  at 1200 °C resulted in specimens having a density of 93% of the theoretical density. Hence, the optimum temperature for sintering of  $\text{Li}_2\text{TiO}_3$  powder derived through the present combustion process is 1100 °C. The high density of sintered specimen of  $\text{Li}_2\text{TiO}_3$  can be attributed to small particle size and higher



**Fig. 6.** Rietveld analysis result of  $\text{Li}_2\text{TiO}_3$  powder. The calculated and observed patterns are shown in the top by the solid line and the dots, respectively. The vertical marks in the middle show positions calculated for Bragg reflection. The trace in the bottom is a plot of the difference: observed minus calculated.



**Fig. 7.** SEM photomicrographs of the fracture surface of  $\text{Li}_2\text{TiO}_3$  specimen sintered at 1050 °C for 90 min.

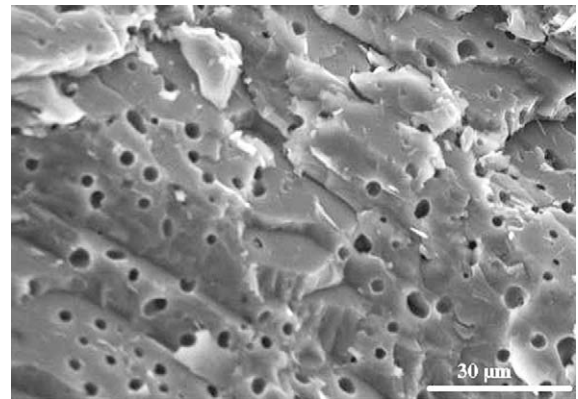


**Fig. 9.** SEM photomicrographs of the fracture surface of  $\text{Li}_2\text{TiO}_3$  specimen sintered at 1150 °C for 90 min.

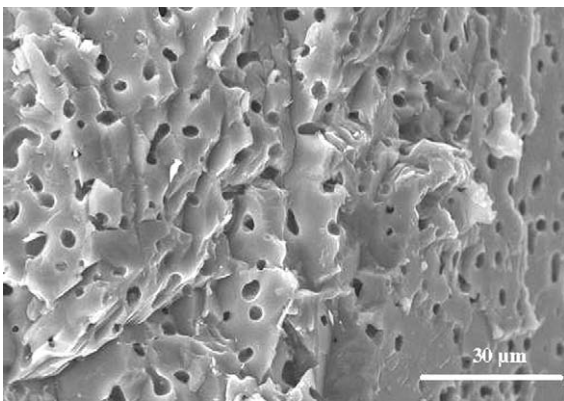


**Fig. 8.** SEM photomicrographs of the fracture surface of  $\text{Li}_2\text{TiO}_3$  specimen sintered at 1100 °C for 90 min.

surface area of starting powder containing nano-crystalline grain as confirmed by XRD.

Fig. 6 shows the Rietveld analysis pattern of  $\text{Li}_2\text{TiO}_3$  that was sintered at 1100 °C. The tick marks below the patterns represent the positions of all possible Bragg reflections. The lower solid line represents the difference between the observed and calculated intensities. The refined lattice parameters of  $\text{Li}_2\text{TiO}_3$  are given in Table 1. The reflections of the pattern correspond to monoclinic polymorph of  $\text{Li}_2\text{TiO}_3$  [ICDD PDF 033-0831]. The quality of the agreement between observed and calculated profiles is evaluated by profile factor ( $R_p$ ), weighted profile factor ( $R_{wp}$ ), expected weighted profile factor ( $R_{exp}$ ), and reduced chi-square ( $\chi^2$ ). The mathematical expressions of the above parameters can be found elsewhere [22]. The reliability parameters obtained through this refinement are  $R_p$ : 10.6%;  $R_{wp}$ : 13.5%;  $R_{exp}$ : 11.25%;  $\chi^2$ : 1.42. The lattice parameters obtained after Rietveld refinements are in good agreement with the reported values of the monoclinic polymorph of  $\text{Li}_2\text{TiO}_3$  [ICDD PDF 033-0831].

The SEM photomicrographs of the fracture surfaces of  $\text{Li}_2\text{TiO}_3$  specimen sintered at 1050–1200 °C are shown in Figs. 7–10. The microstructures of  $\text{Li}_2\text{TiO}_3$  ceramics were found to be uniform. The grains of  $\text{Li}_2\text{TiO}_3$  contained uniformly distributed porosities.



**Table 1**

Lattice parameters and cell volume of  $\text{Li}_2\text{TiO}_3$  phase obtained after Rietveld refinement of XRD data along with similar data from standard pattern of the phase for comparison.

Lattice parameters (Å)/ cell volume (Å <sup>3</sup> )	$\text{Li}_2\text{TiO}_3$ in the present investigation <sup>a</sup>	$\text{Li}_2\text{TiO}_3$ ICDD PDF 033-0831 [23]
<i>a</i>	5.063 (2)	5.069 (2)
<i>b</i>	8.777 (1)	8.799 (7)
<i>c</i>	9.752 (1)	9.759 (9)
$\beta$	100.26 (6)	100.2

<sup>a</sup> Reliability factors after refinement:  $R_p$ : 10.6%;  $R_{wp}$ : 13.5%;  $R_{exp}$ : 11.25%;  $\chi^2$ : 1.42.

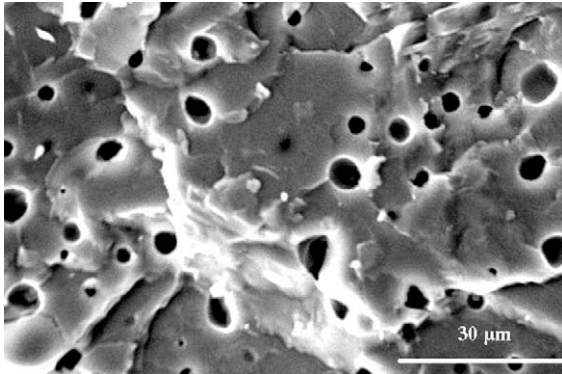


**Fig. 10.** SEM photomicrographs of the fracture surface of  $\text{Li}_2\text{TiO}_3$  specimen sintered at 1200 °C for 90 min.

The average grain size of the sintered specimen increased from 1.6  $\mu\text{m}$  at 1050 °C to 5.82  $\mu\text{m}$  at 1200 °C. Most of the porosities present in the structure of the sintered specimens were closed and the fraction of open porosity was found to be less than 2%. The average diameter of pores increased with sintering temperature from 2  $\mu\text{m}$  at 1050 °C to 5  $\mu\text{m}$  at 1200 °C. All the specimens fracture in trans-granular mode which indicates that the grain boundary strength is higher than that of grain. This could be attributed to the absence of impurity elements along the grain boundary.

#### 4. Conclusion

$\text{Li}_2\text{TiO}_3$  particles were synthesized by a novel solid–liquid combustion synthesis that yields directly the monoclinic phase of  $\text{Li}_2\text{TiO}_3$  after combustion. The process does not call for any additional heat treatment for phase formation. The powder produced through this route could be sintered to 90% of the theoretical density at 1100 °C. The  $\text{Li}_2\text{TiO}_3$  powder produced by the present process seems to be suitable for making high density pebbles for fusion breeder material.

#### References

- [1] E. Proust, L. Anzidei, M.D. Donne, *Fus. Eng. Des.* 16 (1991) 73.
- [2] C.E. Johnson, K.R. Kummerer, E. Roth, *J. Nucl. Mater.* 155–157 (1988) 188.
- [3] N. Roux, J. Avon, A. Floreancig, J. Mougain, B. Rasneur, S. Ravel, *J. Nucl. Mater.* 233–237 (1996) 1431.
- [4] J.M. Miller, H.B. Hamilton, J.D. Sullivan, *J. Nucl. Mater.* 212–215 (1994) 877.
- [5] J.D. Lulewicz, N. Roux, G. Piazza, J. Reimann, J. van der Laan, *J. Nucl. Mater.* 283–287 (2000) 1361.
- [6] J.P. Kopasz, J.M. Miller, C.E. Johnson, *J. Nucl. Mater.* 133&134 (1994) 927.
- [7] O. Renoult, J.P. Boilot, J.P. Korb, M. Boncoeur, *J. Nucl. Mater.* 223 (1995) 126.
- [8] A. Deptula, W. Lada, T. Olczak, A.G. Chmielewski, B. Sartowska, K. Goretta, C. Alvani, *Nukleonika* 46 (3) (2001) 95.
- [9] C. Alvani, P.L. Carconi, S. Casadio, F. Pierdominici, in: J.V. van der Laan (Ed.), *Proceedings of the 7th International Workshop on Ceramic Breeder Blanket Interactions*, Petten, 1998, pp. 4–69–4–80.
- [10] C.H. Jung, J.Y. Park, S.J. Oh, H.K. Park, Y.S. Kim, D.K. Kim, J.H. Kim, *J. Nucl. Mater.* 253 (1998) 203.
- [11] Y. Zhang, G.C. Stangle, *J. Mater. Res.* 9 (1994) 1997.
- [12] S.B. Bhaduri, R. Radhakrishnan, D. Linch, *Ceram. Eng. Sci., Proc.* 15 (1994) 694.
- [13] L.A. Chick, L.R. Pederson, G.D. Maupio, J.L. Bates, *Mater. Lett.* 10 (1990) 6.
- [14] S.R. Jain, K.C. Adigo, V.R. Paiverneker, *Combust. Flame* 40 (1981) 71.
- [15] T. Roisnel, J. Rodríguez-Carvajal, “WinPLOTR: A Windows Tool for Powder Diffraction Patterns Analysis”, *Materials Science Forum*, in: R. Delhez, E.J. Mittemeijer (Eds.), *Proceedings of the Seventh European Powder Diffraction Conference (EPDIC 7)*, 2000, pp. 118–123.
- [16] G. Izquierdo, A.R. West, *Mater. Res. Bull.* 15 (1980) 1655.
- [17] N.S. Landolt-Börnstein, Group III, vol. 7e, Springer, Berlin, 1976.
- [18] J.C. Mikkelsen, *J. Am. Ceram. Soc.* 63 (1980) 331.
- [19] A.U. Christensen, K.C. Conway, K.K. Kelley, Report BMRI-5565, 1960.
- [20] C.-H. Jung, S.J. Lee, W.M. Kriven, J.-Y. Park, W.-S. Ryu, *J. Nucl. Mater.* 373 (2008) 194.
- [21] Y.W. Rhee, J.H. Yang, K.S. Kim, K.W. Kang, K.W. Song, D.J. Kim, *Thermochim. Acta* 455 (2007) 86.
- [22] H.M. Rietveld, *J. Appl. Cryst.* 2 (1969) 65–71. Fullprof. Suite Program. <<http://www.llb.cea.fr/fullweb/fp2k/fp2k.htm>>.
- [23] M. Castellanos, J. West, *J. Mater. Sci.* 14 (1979) 450.